Complex I assembly into supercomplexes determines differential mitochondrial ROS production in neurons and astrocytes

Irene López-Fabuel[1], Juliette Le Douce[2], Angela Logan[3], Andrew M. James[3], Gilles Bonvento[2], Michael P. Murphy[3], Angeles Almeida[4], Juan P. Bolaños[1]

[1]Institute of Functional Biology and Genomics (IBFG), University of Salamanca-CSIC, 37007 Salamanca, Spain; [2]Commissariat à l'Energie Atomique et aux Energies Alternatives (CEA), Département des Sciences du Vivant (DSV), Institut d'Imagerie Biomédicale (I2BM), Molecular Imaging Center (MIRCen), CNRS UMR 9199, Université Paris-Sud, Université Paris-Saclay, F-92260 Fontenay-aux-Roses, France; [3]Medical Research Council Mitochondrial Biology Unit, Wellcome Trust/MRC Building, Cambridge CB2 0XY, United Kingdom; [4]Institute of Biomedical Research of Salamanca (IBSAL), University Hospital of Salamanca, 37007 Salamanca, Spain

Corresponding author:

Prof. Juan P. Bolaños,

Institute of Functional Biology and Genomics (IBFG), University of Salamanca-CSIC,

Zacarias Gonzalez, 2, 37007 Salamanca (Spain)

Phone: +34923294907

E-mail: jbolanos@usal.es

Short title: Different mitochondrial ROS in neurons and astrocytes

Abstract

Neurons depend on oxidative phosphorylation for energy generation, whereas astrocytes do not, a distinctive feature that is essential for neurotransmission and neuronal survival. However, any link between these metabolic differences and the structural organization of the mitochondrial respiratory chain was unknown. Here, we investigated this issue and found that in neurons, mitochondrial complex I is predominantly assembled into supercomplexes, whereas in astrocytes the abundance of free complex I is higher. The presence of free complex I in astrocytes correlates with their several-fold higher reactive oxygen species (ROS) production than that of neurons. Using a complexomics approach, we found that the complex I subunit NDUFS1 was more abundant in neurons than in astrocytes. Interestingly, NDUFS1 knockdown in neurons decreased the association of complex I into supercomplexes, while also leading to impaired oxygen consumption and increased mitochondrial ROS. Conversely, over-expression of NDUFS1 in astrocytes promoted complex I incorporation into supercomplexes while also decreasing ROS. Thus, complex I assembly into supercomplexes correlates with ROS production and may contribute to the bioenergetic differences between neurons and astrocytes.

The brain is a metabolically demanding tissue (1) that requires tight cooperation between neurons and astrocytes (2). Astrocytes are crucial as metabolic and structural support (3, 4) and are also key players in neurotransmission (5-7) and behavior (8 sousa??). The status of many major redox couples in the brain is also regulated by astrocytes (9), through their high content of antioxidant compounds and enzymes (10) and by the constitutive stabilization of the master antioxidant transcriptional activator, nuclear factor-erythroid 2-related factor-2 (Nrf2) (11). Thus, astrocytes are equipped to protect themselves when exposed to excess reactive oxygen species (ROS) (12) and reactive nitrogen reactive species (RNS) (13, 14). Moreover, astrocytes also provide nearby neurons with protective antioxidant precursors through a cell signaling mechanism involving glutamate receptor activation by neurotransmission (11, 15, 16). The tight coupling between astrocytes and neurons therefore helps in energy and redox metabolism during normal brain function.

Intriguingly, the ATP used by neurons is supplied by oxidative phosphorylation, while in contrast most energy needs of astrocytes are met by glycolysis (17). In fact, the very survival of neurons, requires oxidative phosphorylation (18, 19). The different energy metabolisms of the two cell types are closely coupled, with astrocytes releasing the glycolytic end product, lactate, which is used by neighboring neurons to drive oxidtaive phosphorylation (20-22). As the molecular mechanisms underlying the markedly different modes of ATP production in the two cell types is not understood, we investigated whether the organisation of the mitochondrial respiratory chain in brain cells could contribute. Here, we report that the mitochondrial respiratory chain is organized into supercomplexes quite differently in neurons and astrocytes and that

these structural differences correlate with different rates of mitochondrial ROS production and respiration.

RESULTS

More complex I is in supercomplexes in neurons than in astrocytes correlating with mitochondrial function and ROS production

Mitochondrial complexes can organize into supercomplexes in a process that has been claimed to regulate electron transfer efficiency (23). Therefore we assessed whether the structural organization of the mitochondrial respiratory chain differed between neurons and astrocytes. To do this, digitonin-solubilized mitochondria (24) from primary cultures of C57BL/6 mouse neurons and astrocytes were analysed by blue-native gel electrophoresis (BNGE). Complex I occurred both on its own and also bound with complex III, notably in a $I+III_2$ supercomplex and, to a lesser extent, in a I_2+III_2 supercomplex (Fig. 1*A*) (25). The composition of these supercomplexes was confirmed by electro-transfer of the proteins to nitrocellulose followed by immunoblotting against either complex I- (NDUFB8) or complex III- (UQCRC2) (Fig. 1*A*). Interestingly, we observed a significant difference between astrocytes and neurons in the proportion of complex I that was free relative that which was part of a supercomplex, the ratio of free to assembled complex I was higher, whereas the ratio of free to assembled complex III was lower, in astrocytes when compared to neurons (Fig. 1*A*) (see also supporting information (SI) Fig. S*1A*). This pattern of respiratory chain organization was confirmed in freshly isolated neurons and astrocytes (Fig. S*1B,C*) and in cells cultured at 11% O_2, instead of 21% (Fig. S*1D*). The relative abundance of complex I *versus* complex III in astrocytes was twice that in neurons, as judged by western blotting of whole cell extracts (Fig. 1*B*). These data suggest that the relatively low amount of complex III in

astrocytes may limit I-III supercomplex formation, and thereby increase the proportion of complex I in astrocytes that is not present in a supercomplex

To further interrogate the differences in respiratory chain assembly between these two cell typess, we next performed proteomic quantitative analyses of complex I subunits by mass spectrometry of gel slices from BN gels of digitonin-solubilized mitochondria from astrocytes or neurons. As shown in Fig. 1*C*, measurement of complex I subunits showed that the amounts of these subunits present in free complex I, relative to those present in $I+III_2$ plus I_2+III_2 supercomplexes, was about 2-fold greater in astrocytes compared to neurons. This was further assessed by assaying rotenone-sensitive NADH-ubiquinone oxidoreductase activity in proteins electroeluted from BN gel slices containing the supercomplexes or free (CI) complex I. . This showed that, the NADH-ubiquinone oxidoreductase activity in the free complex I band was higher in astrocytes than in neurons (Fig. 1*D*). Since complex I catalyzes $O_2^{\bullet-}$ production (26), we next determined $O_2^{\bullet-}$ in an in-gel $O_2^{\bullet-}/H_2O_2$ coupled assay in complex I-containing slices excised from the BNGE, and we found that ROS production from the free complex I band was higher in astrocytes than in neurons (Fig. 1*E*). I still don't like this assay!...I'd delete it, but up to you. These results confirm that the ratio of free complex I to that present in supercomplexes is higher in astrocytes than it is in neurons.

Since the organization of respiratory complexes into supercomplexes is claimed to affect mitochondrial function and ROS production (23, 25), we next determined O_2 consumption in mitochondria isolated from astrocytes and neurons. As shown in Fig. 1*F*, state 3 pyruvate/malate-driven O_2 consumption in astrocytes was nearly half that in neurons. To ascertain if there were any differences in mitochondrial ROS production

between these tow cell types, we also determined the rate of H_2O_2 formation in isolated mitochondria. As shown in Fig. 1*G*, mitochondrial ROS production was higher in mitochondria from astrocytes than from neurons, either from endogenous substrates or in the presence of pyruvate/malate. Thus, the different of complex I presence in supercomplexes in the respiratory chain of mitochondria in neurons and astrocytes correlates with differences in mitochondrial function and ROS production.

Astrocytes produce more mitochondrial ROS than neurons

To see if the differences in ROS production by mitochondria isolated from neurons and astrocytes occurred in intact cells, we determined the rate of H_2O_2 generation by intact neurons and astrocytes in primary cultures isolated from the brains of mice and rats. Astrocytes produced H_2O_2 about one order of magnitude faster than neurons, fro both rat and mouse and under all culture conditions investigated (Fig. 2*A*; Fig. S*2A-C*). We next assessed mitochondrial ROS production (27) using the mitochondria-targeted probes MitoSox™ and MitoB (28) in intact cells. The MitoSox™ fluorescence and the MitoP/MitoB ratio were higher in astrocytes than in neurons (Fig. 2*B,C*; Fig. S*2E-H*), indicating an elevation of mitochondrial ROS in astrocytes compared to neurons under these conditions. Interestingly, the differences in MitoSox™ fluorescence and in mitochondrial H_2O_2 production, between neurons and astrocytes, were unchanged after $\Delta\psi_m$ disruption with CCCP (Fig. 2*D,E*), suggestingthat the difference is not a possible artifact due to their different $\Delta\psi_m$ affecting probe distribution.

I WASN'T CLEAR IF CCP DECREASED THE AMOUNT OF ROS BUT THAT THERE WAS STILL A DIFFERENCE BETWEEN ASTROCYTES AND NEURONS, OR THAT CCCP HAD NO EFFECT ON ROS? Other non-mitochondrial ROS sources,

such as xanthine oxidase, NADPH oxidases and nitric oxide synthase, did not appear to contribute to the high rate of ROS production in astrocytes (Fig. S*3A-E*).

Thus, we conclude that mitochondrial ROS production is greater in astrocytes than in neurons.

We next investigated mitochondrial ROS production in neurons and astrocytes acutely dissociated from the mouse brain. For this brain cells were isolated from mice previously stereotaxically-injected with adeno-associated viruses expressing green fluorescence protein (GFP) under the control of either an astrocyte or a neuronal specific promoter. Cells were then subjected to mitochondrial ROS assessment by flow cytometry analysis using MitoSox™. As shown in Fig. 2*F*, the MitoSox™ fluorescence was higher in astrocyte promoter-driven GFP^+ cells (expressing the astrocyte specific Glial-Fibrillary Acidic Protein or GFAP) than in neuron promoter-driven GFP^+ cells (expressing the neuron specific Neuronal Nuclei or NeuN). Moreover, freshly isolated mouse brain cells, sorted according to the astrocyte-specific plasma membrane protein, integrin ß5 (29) showed a similar difference in ROS (Fig. S4*A,B*). Finally, we found that the rate of mitochondrial ROS production was higher in astrocytes than in neurons freshly purified from the mouse brain using MACS® technology (Fig. S*5C*). Thus, astrocytes produce mitochondrial ROS several-fold faster than neurons.

High ROS production by astrocytes correlates with deactive complex I

Given that complex I is a major source of mitochondrial ROS is (27), we analyzed the specific activity of complex I in neurons and in astrocytes. As shown in Fig. 3*A*, complex I activity was very similar in both cell types, as were the activities of other respiratory chain complexes (Fig. S*5A*). The complex I inhibitor, rotenone, stimulated

mitochondrial ROS production to a great extent in neurons, but only slightly stimulated in astrocytes; however, antimycin stimulated mitochondrial ROS production in both cell types (Fig. 2*D*). The mild effect of rotenone on mitochondrial ROS production in astrocytes was intriguing as rotenone stimulates forward (FET) and inhibits the reverse (RET) electron transfer to O_2 at complex I (26, 29), suggesting that RET-mediated ROS is negligible in astrocytes (Fig. S*5B,C*). Since the ubiquinone binding site is inaccessible in deactive complex I (30, 31), rendering it insensitive to rotenone, we hypothesized whether there were different proportions of deactive and active complex I in neurons and astrocytes. As shown in Fig. 3*B* (see, also, Fig. S*5D*), the proportion of deactive complex I is one third (~33%) of total complex I in astrocytes, but only ~5% in neurons. Given that deactive complex I preferentially transfers electrons to O_2 instead of to ubiquinone (30, 31), our results suggest that the high proportion of deactive free complex I in astrocytes may contribute to the higher mitochondrial ROS production of these cells.

Modulation of complex I assembly into supercomplexes alters ROS production and respiration in neurons and astrocytes

To see whether ROS production and respiration are affected by the proportion of complex I incorporated in to supercomplexes, we first assessed the relative abundance of complex I subunits in complex I-containing bands from the BNGE gel. The majority of complex I subunits were asymmetrically distributed, both in astrocytes and in neurons (Fig. 3*C*). This is consistent with recent work showing different states of subcomplex I aggregates in aging (32). Interestingly, we observed that the only complex I subunit that was distributed equally in both cell types was NUDFS1 (Fig. 3*C*), which harbors three out of the eight Fe-S clusters of complex I (33). Given its essential role in

electron transfer, we next assessed the NDUFS1 protein abundance. NDUFS1 protein abundance was higher in neurons than in astrocytes, as judged by BNGE followed by immunoblotting directly, or after second dimension SDS-PAGE (Fig. *3D*). We found that NDUFS1 knockdown in neurons (Fig. 4*A*) diminished free and supercomplex-assembled complex I abundance (Fig. 4*B,C*). Consistent with this, ROS production increased in free complex I and in complex I-containing supercomplexes bands excised from the BNGE gel (Fig. 4*D*)delete?, and in the intact NDUFS1-silenced neurons (Fig. 4*E*). These effects impaired the electron transfer efficiency through the mitochondrial respiratory chain, as judged by the decreased pyruvate/malate-driven O_2 consumption in isolated mitochondria (Fig. 4*F*). Conversely, NDUFS1 overexpression in astrocytes (Fig. 5*A*) increased free complex I and promoted its assembly into supercomplexes (Fig. 5*B,C*). Consistent with this, ROS production decreased by free and complex I-containing supercomplexes excised from the BNGE gel (Fig. 5*D*), as well as delet? in the intact NDUFS1-overexpressing astrocytes (Fig. 5*E*). This was not associated, however, with an increase in pyruvate/malate-driven O_2 consumption (Fig. 5*F*), which is consistent with the low abundance of complex III in astrocytes that limits electron transference to O_2 (Fig. 1*B*). Thus, modulation of complex I assembly into supercomplexes can affect mitochondrial O_2 consumption and ROS production.

DISCUSSION

Here, we describe that neurons and astrocytes have organize their mitochondrial respiratory chains differently in the proportion of complex I that is free or present in supercomplexes. In astrocytes, complex I is loosely assembled into supercomplexes, leaving more free complex I (34). In contrast, in neurons more of the complex I is assembled into supercomplexes. These differences correlate with changes in ROS

production and respiration, with themore free complex I segregating with elevated ROS production. These rates of mitochondrial ROS formation are altered by re-organizing the mitochondrial respiratory chain by increasing or decreasing the level of NDUFS1. Interestingly, the rate of ROS formation inversely correlated with electron transfer efficiency in neurons, with NDUFS1 knockdown impairing mitochondrial O_2 consumption but increasing ROS. In contrast, NDUFS1 over-expression in astrocytes decreased ROS, although it did not increase mitochondrial O_2 consumption. This effect of complex I abundance can be explained by the reduced abundance of complex III in astrocytes that limits the amount of complex I that can be sequestred into supercomplexes.

Our results may help explain the different redox and bioenergetics features of neurons and astrocytes. Thus, the greater proportion of complex I that is assembled into supercomplexes in neurons may contribute to the higher respiration rate of neurons compared to astrocytes, and is consistent with the dependence of neurons on oxidative phosphorylation for neurotransmission and survival (17-19). In contrast, the smaller proportion of complex I that is assembled into supercomplexes in astrocytes may contribute to their lower respiration rate and be an adaptation to a more glycolytic metabolism (17-22). A further intriguing aspect was that the large difference in mitochondrial ROS production between also correlated with the amount of complex I that was not present in supercomplexes. This may explain why astrocytes produce more ROS than neurons, and hence are equipped with a robust redox antioxidant system (35, 36). Indeed, astrocytes express functionally active Nrf2 (11), a transcription factor that is activated by ROS (37) and governs the expression of a plethora of antioxidant genes aimed to protect themselves and also neighboring neurons (38).

In conclusion, our data suggest that the extent of assembly of complex I into supercomplexes is different between in neurons and astrocytes and contributes to some of the differences in ROS and mitochondrial metabolism between these cells. However, the functional and mechanistic role of supercomplexes is currently unclear and disputed (REFERENCE JUDY'S paper in PNAS). In future work it will be important to determine the mechanism(s) underlying the changes in respiration and ROS between neurons and astrocytes. In particular it will be important to determine whether these differences are due to the properties of the supercomplexes themselves, or whether the balance between the relative levels of complexes I and III is more critical. Furthermore, it will be very interesting to explore whether changes in complex I incorporatioin into supercomplexes and/or its balance with complex III contribute to excessive ROS associated in pathological situations such as in the dopaminergic neuronal death in Parkinson's disease (PD) (39-41) and whether interventions aimed at maintaining complex I stability would be a promising therapeutic approach against this, and other neurodegenerative diseases.

MATERIALS AND METHODS

Ethical use of animals. Wistar rats and C57BL/6 mice were bred at the Animal Experimentation Unit of the University of Salamanca. All protocols were approved by the Bioethics Committee of the University of Salamanca in accordance with the Spanish legislation (Law 6/2013).

Primary cell cultures. Primary cultures of Wistar rat or C57BL/6 mouse cortical neurons and astrocytes were prepared from embryonic day 15.5-16.5 (neurons) or postnatal 0-24 h (astrocytes), as described previously (42) (see also *SI Text*).

Mitochondria isolation and solubilization. Mitochondria were isolated according to a previously published protocol (24) and solubilized with digitonin at 4 g/g (5 minutes in ice) (*SI Text*).

Mitochondrial respiration. To measure the state III oxygen consumption rates, we used a Clark-type electrode (Rank Brothers). Neuronal and astrocytic cells were recollected by trypsinization and mitochondria were immediately obtained. Freshly-isolated mitochondria (100 µg) were suspended in the respiration medium (KCl 125 mM; KH_2PO_4 2 mM; $MgCl_2$ 1 mM; BSA 0.5 mg/ml; HEPES 10 mM; pH 7.4). Oxygen consumption was determined after the addition of 5 mM of pyruvate plus 5 mM of malate (state II), followed by the addition of 1 mM of ADP (state III).

ROS determination. Mitochondrial ROS was detected using the fluorescent probe MitoSox™ (Life Technologies) and MitoB probe (*SI Text*). For H_2O_2 assessments, AmplexRed™ (Life Technologies) was used (*SI Text*). H_2O_2 measured directly form blue native gel electrophoresis (BNGE) gel slices were performed in the presence of 20 µM of NADH and 40 U/ml of SOD (SI Text).

Mitochondrial membrane potential. The mitochondrial membrane potential ($\Delta\underline{\psi}_m$) was assessed using the probe DiIC1(5) (Life Technologies) (50 nM) by flow cytometry *(SI Text*).

Activity of mitochondrial complexes. Cells were collected and suspended in PBS (pH 7.0). After three cycles of freeze/thawing, to ensure cellular disruption, complex I, complex II, complex II-III, complex IV and citrate synthase activities were determined spectrophotometrically as indicated in *SI Text*.

Blue native gel electrophoresis (BNGE). For the assessment of complex I organization, digitonin solubilized mitochondria (10-50 μg) were loaded in NativePAGE Novex 3-12% gels (Life Technologies). After electrophoresis, in-gel NADH dehydrogenase activity was evaluated (43). After identification of individual complex I and complex I-containing supercomplexes bands according to the NADH dehydrogenase activity, either a direct electro-transfer or a second dimension (2D) sodium dodecyl sulphate (SDS)-polyacrylamide gel electrophoresis (PAGE) were performed to identify some subunits of the mitochondrial complexes. Thus, individual complex I or complex I-containing supercomplexes bands were excised from the gel and denatured in 1% SDS (containing 1 % β-mercaptoethanol) during 1 hour. The proteins contained in the gel slices were separated electrophoretically, followed by Western blotting against NDUFS1 or NDUFV1 specific antibodies. Coomassie staining of BNGE gels was performed, as an indicator of loaded protein, during 15 minutes followed by different steps of destaining with 10% (v/v) acetic acid *plus* 20% (v/v) methanol. Direct transfer of BNGE was performed after soaking the gels for 20 minutes (4ºC) in carbonate buffer (10 mM $NaHCO_3$, 3 mM $Na_2CO_3 \cdot 10H_2O$, pH 9.5-10). Proteins transfer to nitrocellulose membranes was carried out at 300 mA, 60 V, 1 hour at 4ºC in carbonate buffer.

Electroelution of proteins. Following BNGE and in-gel NADH dehydrogenase activity, individual and complex I-containing supercomplexes bands were excised, and the proteins electroeluted. To electroelute proteins, gel slices were placed in an electrodialysis membrane (Dialysis Tubing-Visking, Medicall International), and an electric field was applied during 4 h at 100 V. The samples containing the electroeluted proteins were collected, and the complex I specific activity determined.

Mass spectrometry. Mass spectrometry analysis was carried out in the BNGE gel slices excised from the individual complex I, complex I-containing supercomplexes, and in the inter-bands, at the MRC Mitochondrial Biology Unit (Cambridge) as described in *SI Text*.

Protein determinations. Protein samples were quantified by the BCA protein assay kit (Thermo) following the manufacturer's instructions, using BSA as a standard.

Statistical analysis. All measurements were carried out at least in three different culture preparations or animals, and the results were expressed as the mean values ± SEM. For the comparisons between two groups of values, the statistical analysis of the results was performed by the Student's *t* test. For multiple values comparisons, we used one-way analysis of variance (ANOVA) followed by Bonferroni test. The statistical analysis was performed using the SPSS software. In all cases, $p<0.05$ was considered significant.

REFERENCES

1. Magistretti PJ (2006) Neuron-glia metabolic coupling and plasticity. *J Exp Biol* 209**:**2304-11.
2. Allen NJ, Barres, BA (2009) Neuroscience: Glia - more than just brain glue. *Nature* 457**:**675-7.

3. Kimelberg HK, Nedergaard, M (2010) Functions of astrocytes and their potential as therapeutic targets. *Neurotherapeutics* 7**:**338-53.
4. Perea G, Sur, M, Araque, A (2014) Neuron-glia networks: integral gear of brain function. *Front Cell Neurosci* 8**:**378.
5. Parpura V, Basarsky, TA, Liu, F, Jeftinija, K, Jeftinija, S, Haydon, PG (1994) Glutamate-mediated astrocyte-neuron signalling. *Nature* 369**:**744-7.
6. Perea G, Navarrete, M, Araque, A (2009) Tripartite synapses: astrocytes process and control synaptic information. *Trends Neurosci* 32**:**421-31.
7. Araque A, Carmignoto, G, Haydon, PG, Oliet, SH, Robitaille, R, Volterra, A (2014) Gliotransmitters travel in time and space. *Neuron* 81**:**728-39.
8. Oliveira JF, Sardinha, VM, Guerra-Gomes, S, Araque, A, Sousa, N (2015) Do stars govern our actions? Astrocyte involvement in rodent behavior. *Trends Neurosci* 38**:**535-49.
9. Schreiner B, Romanelli, E, Liberski, P, Ingold-Heppner, B, Sobottka-Brillout, B, Hartwig, T, Chandrasekar, V, Johannssen, H, Zeilhofer, HU, Aguzzi, A, Heppner, F, Kerschensteiner, M, Becher, B (2015) Astrocyte Depletion Impairs Redox Homeostasis and Triggers Neuronal Loss in the Adult CNS. *Cell Rep* 12**:**1377-84.
10. Makar TK, Nedergaard, M, Preuss, A, Gelbard, AS, Perumal, AS, Cooper, AJL (1994) Vitamin E, ascorbate, glutathione, glutathione disulfide, and enzymes of glutathione metabolism in cultures of chick astrocytes and neurones: evidence that astrocytes play an important role in antioxidative processes in the brain. *J Neurochem* 62**:**45-53.
11. Jimenez-Blasco D, Santofimia-Castano, P, Gonzalez, A, Almeida, A, Bolanos, JP (2015) Astrocyte NMDA receptors' activity sustains neuronal survival through a Cdk5-Nrf2 pathway. *Cell Death Differ* 22**:**1877-89.
12. Dringen R, Pfeiffer, B, Hamprecht, B (1999) Synthesis of the antioxidant glutathione in neurons: supply by astrocytes of CysGly as precursor for neuronal glutathione. *J Neurosci* 19**:**562-569.
13. Bolaños JP, Heales, SJR, Land, JM, Clark, JB (1995) Effect of peroxynitrite on the mitochondrial respiratory chain: differential susceptibility of neurones and astrocytes in primary cultures. *J Neurochem* 64**:**1965-1972.

14. Bolaños JP, Heales, SJR, Peuchen, S, Barker, JE, Land, JM, Clark, JB (1996) Nitric oxide-mediated mitochondrial damage: a potential neuroprotective role for glutathione. *Free Rad Biol Med* 21**:**995-1001.
15. Deighton RF, Markus, NM, Al-Mubarak, B, Bell, KF, Papadia, S, Meakin, PJ, Chowdhry, S, Hayes, JD, Hardingham, GE (2014) Nrf2 target genes can be controlled by neuronal activity in the absence of Nrf2 and astrocytes. *Proc Natl Acad Sci U S A* 111**:**E1818-20.
16. Baxter PS, Bell, KF, Hasel, P, Kaindl, AM, Fricker, M, Thomson, D, Cregan, SP, Gillingwater, TH, Hardingham, GE (2015) Synaptic NMDA receptor activity is coupled to the transcriptional control of the glutathione system. *Nat Commun* 6**:**6761.
17. Almeida A, Moncada, S, Bolaños, JP (2004) Nitric oxide switches on glycolysis through the AMP protein kinase and 6-phosphofructo-2-kinase pathway. *Nat Cell Biol* 6**:**45-51.
18. Almeida A, Almeida, J, Bolaños, JP, Moncada, S (2001) Different responses of astrocytes and neurons to nitric oxide: the role of glycolytically-generated ATP in astrocyte protection. *Proc Natl Acad Sci USA* 98**:**15294-15299.
19. Herrero-Mendez A, Almeida, A, Fernandez, E, Maestre, C, Moncada, S, Bolaños, JP (2009) The bioenergetic and antioxidant status of neurons is controlled by continuous degradation of a key glycolytic enzyme by APC/C-Cdh1. *Nat Cell Biol* 11**:**747-52.
20. Pellerin L, Magistretti, PJ (1994) Glutamate uptake into astrocytes stimulates aerobic glycolysis: a mechanism coupling neuronal activity to glucose utilization. *Proc Natl Acad Sci U S A* 91**:**10625-9.
21. Bouzier-Sore AK, Voisin, P, Canioni, P, Magistretti, PJ, Pellerin, L (2003) Lactate is a preferential oxidative energy substrate over glucose for neurons in culture. *J Cereb Blood Flow Metab* 23**:**1298-306.
22. Allaman I, Belanger, M, Magistretti, PJ (2011) Astrocyte-neuron metabolic relationships: for better and for worse. *Trends Neurosci* 34**:**76-87.
23. Bianchi C, Genova, ML, Parenti Castelli, G, Lenaz, G (2004) The mitochondrial respiratory chain is partially organized in a supercomplex assembly: kinetic evidence using flux control analysis. *J Biol Chem* 279**:**36562-9.
24. Acin-Perez R, Fernandez-Silva, P, Peleato, ML, Perez-Martos, A, Enriquez, JA (2008) Respiratory active mitochondrial supercomplexes. *Mol Cell* 32**:**529-39.

25. Lapuente-Brun E, Moreno-Loshuertos, R, Acin-Perez, R, Latorre-Pellicer, A, Colas, C, Balsa, E, Perales-Clemente, E, Quiros, PM, Calvo, E, Rodriguez-Hernandez, MA, Navas, P, Cruz, R, Carracedo, A, Lopez-Otin, C, Perez-Martos, A, Fernandez-Silva, P, Fernandez-Vizarra, E, Enriquez, JA (2013) Supercomplex assembly determines electron flux in the mitochondrial electron transport chain. *Science* 340**:**1567-70.

26. Kussmaul L, Hirst, J (2006) The mechanism of superoxide production by NADH:ubiquinone oxidoreductase (complex I) from bovine heart mitochondria. *Proc Natl Acad Sci U S A* 103**:**7607-12.

27. Murphy MP (2009) How mitochondria produce reactive oxygen species. *Biochem J* 417**:**1-13.

28. Cocheme HM, Quin, C, McQuaker, SJ, Cabreiro, F, Logan, A, Prime, TA, Abakumova, I, Patel, JV, Fearnley, IM, James, AM, Porteous, CM, Smith, RA, Saeed, S, Carre, JE, Singer, M, Gems, D, Hartley, RC, Partridge, L, Murphy, MP (2011) Measurement of H2O2 within living Drosophila during aging using a ratiometric mass spectrometry probe targeted to the mitochondrial matrix. *Cell Metab* 13**:**340-50.

29. Foo LC (2013) Purification of rat and mouse astrocytes by immunopanning. *Cold Spring Harb Protoc* 2013**:**421-32.

30. Babot M, Labarbuta, P, Birch, A, Kee, S, Fuszard, M, Botting, CH, Wittig, I, Heide, H, Galkin, A (2014) ND3, ND1 and 39kDa subunits are more exposed in the de-active form of bovine mitochondrial complex I. *Biochim Biophys Acta* 1837**:**929-39.

31. Roberts PG, Hirst, J (2012) The deactive form of respiratory complex I from mammalian mitochondria is a Na+/H+ antiporter. *J Biol Chem* 287**:**34743-51.

32. Miwa S, Jow, H, Baty, K, Johnson, A, Czapiewski, R, Saretzki, G, Treumann, A, von Zglinicki, T (2014) Low abundance of the matrix arm of complex I in mitochondria predicts longevity in mice. *Nat Commun* 5**:**3837.

33. Janssen RJ, Nijtmans, LG, van den Heuvel, LP, Smeitink, JA (2006) Mitochondrial complex I: structure, function and pathology. *J Inherit Metab Dis* 29**:**499-515.

34. Maranzana E, Barbero, G, Falasca, AI, Lenaz, G, Genova, ML (2013) Mitochondrial respiratory supercomplex association limits production of reactive oxygen species from complex I. *Antioxid Redox Signal* 19**:**1469-80.

35. Diaz-Hernandez JI, Almeida, A, Delgado-Esteban, M, Fernandez, E, Bolanos, JP (2005) Knockdown of glutamate-cysteine ligase by small hairpin RNA reveals that both catalytic and modulatory subunits are essential for the survival of primary neurons. *J Biol Chem* 280**:**38992-39001.
36. Fernandez-Fernandez S, Almeida, A, Bolanos, JP (2012) Antioxidant and bioenergetic coupling between neurons and astrocytes. *Biochem J* 443**:**3-11.
37. Tebay LE, Robertson, H, Durant, ST, Vitale, SR, Penning, TM, Dinkova-Kostova, AT, Hayes, JD (2015) Mechanisms of activation of the transcription factor Nrf2 by redox stressors, nutrient cues, and energy status and the pathways through which it attenuates degenerative disease. *Free Radic Biol Med***:**FRBMD1500379.
38. Johnson DA, Johnson, JA (2015) Nrf2-a therapeutic target for the treatment of neurodegenerative diseases. *Free Radic Biol Med*.
39. Perry TL, Godin, DV, Hansen, S (1982) Parkinson's disease: a disorder due to nigral glutathione deficiency? *Neurosci Lett* 33**:**305-310.
40. Schapira AH, Cooper, JM, Dexter, D, Jenner, P, Clark, JB, Marsden, CD (1989) Mitochondrial complex I deficiency in Parkinson's disease. *Lancet* 1**:**1269.
41. Schapira AH (2012) Mitochondrial diseases. *Lancet* 379**:**1825-34.
42. Requejo-Aguilar R, Lopez-Fabuel, I, Fernandez, E, Martins, LM, Almeida, A, Bolanos, JP (2014) PINK1 deficiency sustains cell proliferation by reprogramming glucose metabolism through HIF1. *Nat Commun* 5**:**4514.
43. Diaz F, Barrientos, A, Fontanesi, F (2009) Evaluation of the mitochondrial respiratory chain and oxidative phosphorylation system using blue native gel electrophoresis. *Curr Protoc Hum Genet* Chapter 19**:**Unit19 4.

Conflict of Interest

The authors declare no conflict of interest.

Acknowledgements

J.P.B. is funded by the MINECO (SAF2013-41177-R), the Instituto de Salud Carlos III (RD12/0043/0021), the E.U. SP3-People-MC-ITN programme (608381), the EU

BATCure grant (666918), and the NIH/NIDA (1R21DA037678-01). A.A.P. is funded by the Instituto de Salud Carlos III (PI12/00685 and RD12/0014/0007). We acknowledge Monica Carabias and Monica Resch for technical assistances, Noëlle Dufour, Charlène Joséphine and Alexis Bemelmans for AAVs production, and Charlène Joséphine, Martine Guillermier, Diane Houitte and Gwenaëlle Aurégan for stereotaxic injections of AAVs.

Author contributions

JPB conceived the idea and planned the experiments. ILB, JLD, GB, AMJ, MPM and AA designed and performed research and analyzed the data. JPB wrote the manuscript.

Fig. 1 - Lopez-Fabuel et al.

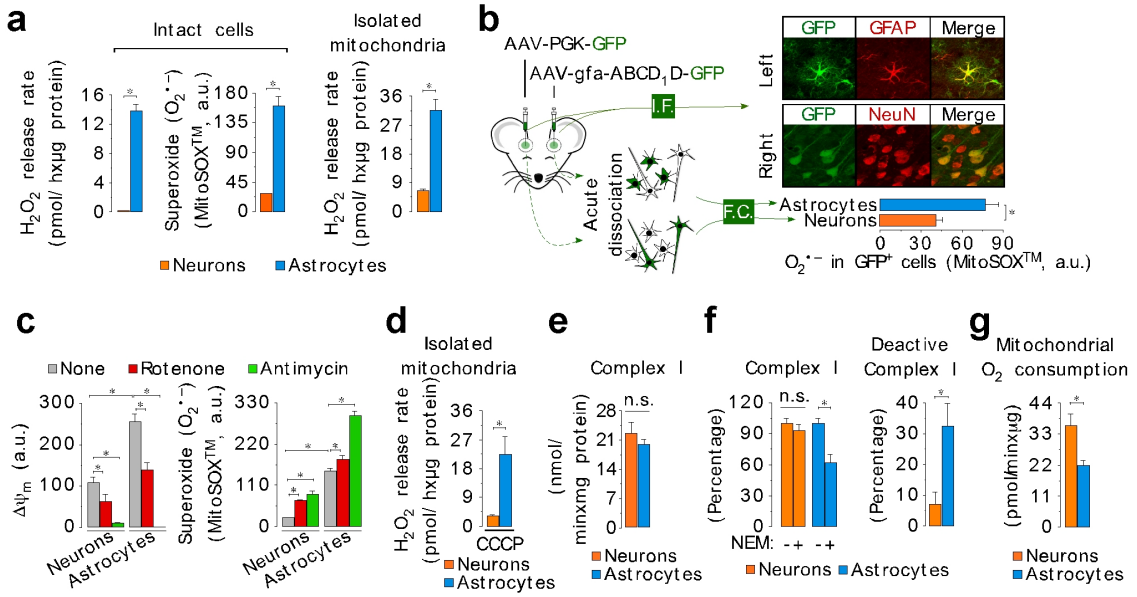

Fig. 1. Different assembly of complex I into supercomplexes between neurons and astrocytes correlates with ROS production and mitochondrial respiration

(*A*) Digitonin-solubilized isolated mitochondria from mouse astrocytes and neurons were subjected to blue-native gel electrophoresis (BNGE) followed by in-gel complex I activity assay. Complex I occurs both free and bound with complex III ($I+III_2$ and I_2+III_2 supercomplexes). Direct electro-transfer of the native proteins to nitrocellulose followed by immunoblotting against NDUFB8 (a complex I subunit) or UQCRC2 (a complex III subunit). **(*B*)** Western blotting against NDUFB8 and UQCRC2 in whole cell protein extracts showing the relative abundance of complex I *versus* complex III in astrocytes and neurons. **(*C*)** Slices were excised from digitonin-solubilized isolated astrocyte and neuronal mitochondria BNGE gels, and the abundances of complex I subunits in free complex I (CI), relative to the abundance of those in $I+III_2$ and I_2+III_2 supercomplexes (SC), were assessed by complexomics. **(*D*)** Rotenone-sensitive NADH-ubiquinone oxidoreductase activity of the excised and electroeluted free complex I and complex I-supercomplexes bands from the BNGE gel in astrocytes and neurons. Data were not normalized per protein abundance in the eluate, as we aimed to assess the

amount of total complex I activity present in each band. **(*E*)** In-gel H_2O_2 production in the excised SC and CI bands from the BNGE in astrocytes and neurons. H_2O_2 production values were normalized by the NADH dehydrogenase-activity band intensity obtained in the BNGE. **(*F*)** Pyruvate/malate (5 mM each)-driven mitochondrial oxygen consumption in isolated mitochondria from neurons or astrocytes under state III (1 mM ADP). **(*G*)** Rate of H_2O_2 production assessed using the AmplexRed™ assay, in mitochondria isolated from neurons and astrocytes, in the presence and absence of pyruvate/malate (5 mM each). Data are the mean values ± S.E.M. from n=3-4 independent culture preparations (Student's t test; ANOVA post-hoc Bonferroni). *p<0.05.

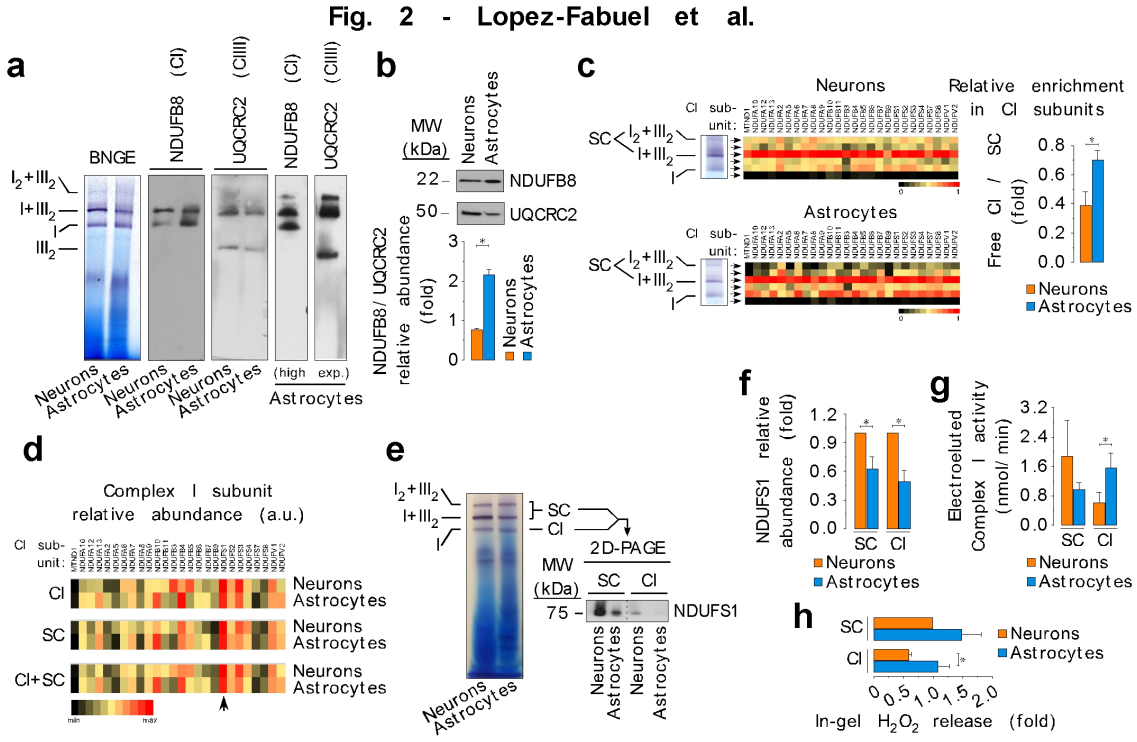

Fig. 2. Higher mitochondrial ROS production in astrocytes than in neurons occurs *ex vivo*

(*A*) Rates of H_2O_2 production assessed using the AmplexRed™ assay, in intact C56BL/6 mouse neurons and astrocytes in primary culture. **(*B*)** Mitochondrial ROS was

quantified using the MitoSox™ assay in the intact cells (C57BL/6) by flow cytometry. **(*C*)** Mitochondrial ROS levels assessed using MitoB probe. Ratio between MitoP (oxidized form) *versus* MitoB is normalized per million of cells. **(*D*)** Mitochondrial membrane potential ($\Delta\psi_m$) (left panel) and MitoSox™ fluorescence (right panel) were determined in basal conditions and after the inhibition of complex I (rotenone) or complex III (antimycin). Rotenone or antimycin was used at 10 µM, each, for 15 min. Furthermore, MitoSox™ fluorescence was evaluated after cell preincubation with the uncoupler CCCP (10 µM, 15 min) **(*E*)** Mitochondrial H_2O_2 production after $\Delta\psi_m$ abolishment with the uncoupler CCCP (10 µM, 15 min). **(*F*)** Mitochondrial ROS abundance (MitoSox™) assessed by flow cytometry (FC) in freshly isolated neurons and astrocytes from adult brain mouse expressing GFP governed either by an astrocyte (gfa-ABC_1D) or a neuronal (PGK) promoter. Cell-specificity of promoter-driven GFP expression was validated by immunofluorescence (I.F.) microscopy using astrocyte (GFAP) or neuronal (NeuN) markers (40X magnification). Data are the mean values ± S.E.M. from n=3-4 independent culture preparations or n=8 animals (Student's *t* test; ANOVA post-hoc Bonferroni). *$p<0.05$.

Fig. 3 - Lopez-Fabuel et al.

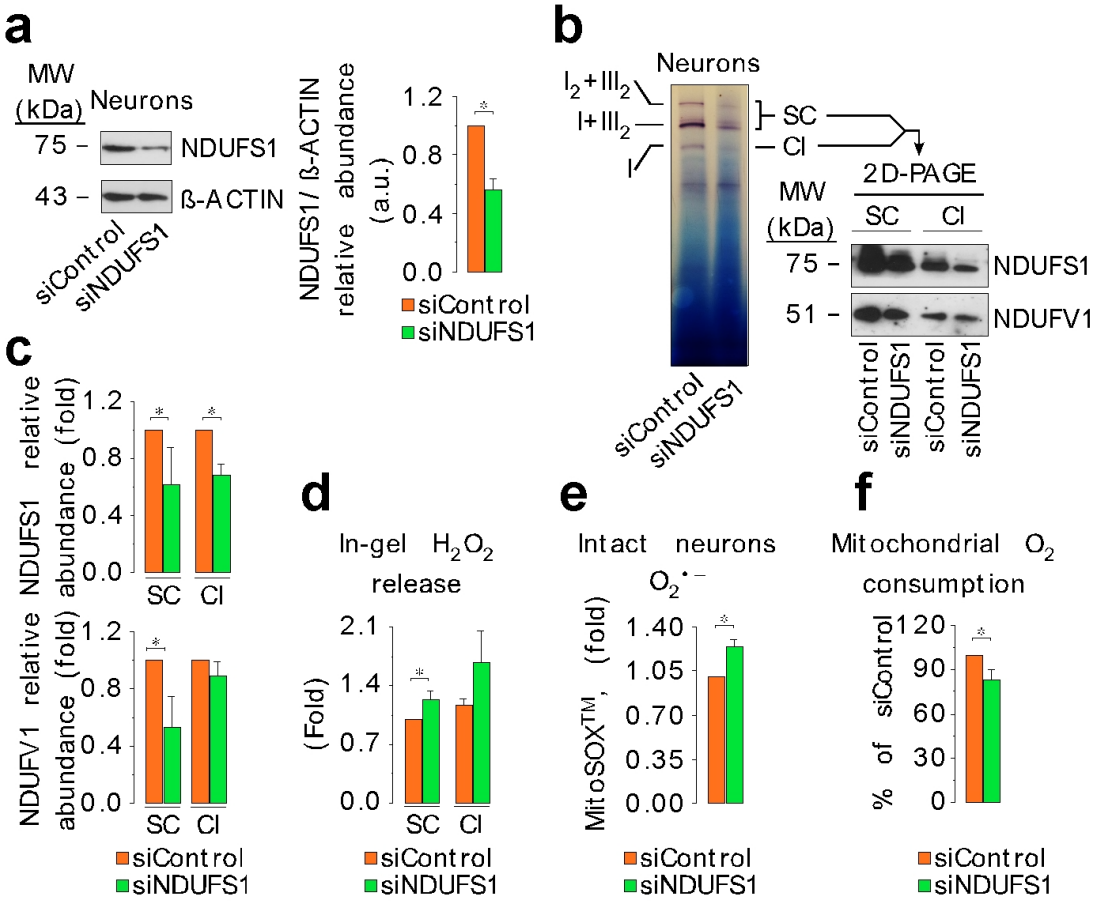

Fig. 3. Astrocytes present high proportion of deactive complex I, with a reduced abundance of NDUFS1 subunit

(*A*) Mitochondrial complex I (rotenone-sensitive NADH-ubiquinone oxidorreductase) activity, as assessed spectrophotometrically in cell homogenates, in astrocytes and neurons. **(*B*)** Deactive complex I activity, as assessed by the difference in rotenone-sensitive NADH-ubiquinone oxidorreductase activity obtained with or without N-ethylmaleimide (NEM, 10 mM) in astrocytes and neurons. **(*C*)** Complex I subunits, excised from complex I-containing bands from a BNGE gel, were rated according to their signal intensities. The arrow indicates the most easily observed complex I subunit (NDUFS1) present both in free and in bound (supercomplexes) complex I fractions in neurons and astrocytes. **(*D*)** NDUFS1 protein abundance in neurons and astrocytes, as assessed by BNGE either followed by direct electro-blotting (also with complex III-

UQCRC2 *plus* complex IV-MT-CO1 subunits) or by second dimension SDS-PAGE immunoblotting followed by densitometric band intensity quantification. Coomassie stained proteins from the BNGE was used as loading control. CIII: complex III subunit UQCRC2; CIV: complex IV subunit MT-CO1. Data are the mean values ± S.E.M. from n=3-4 independent culture preparations or n=8 animals (Student's t test). *p<0.05.

Fig. 4 - Lopez-Fabuel et al.

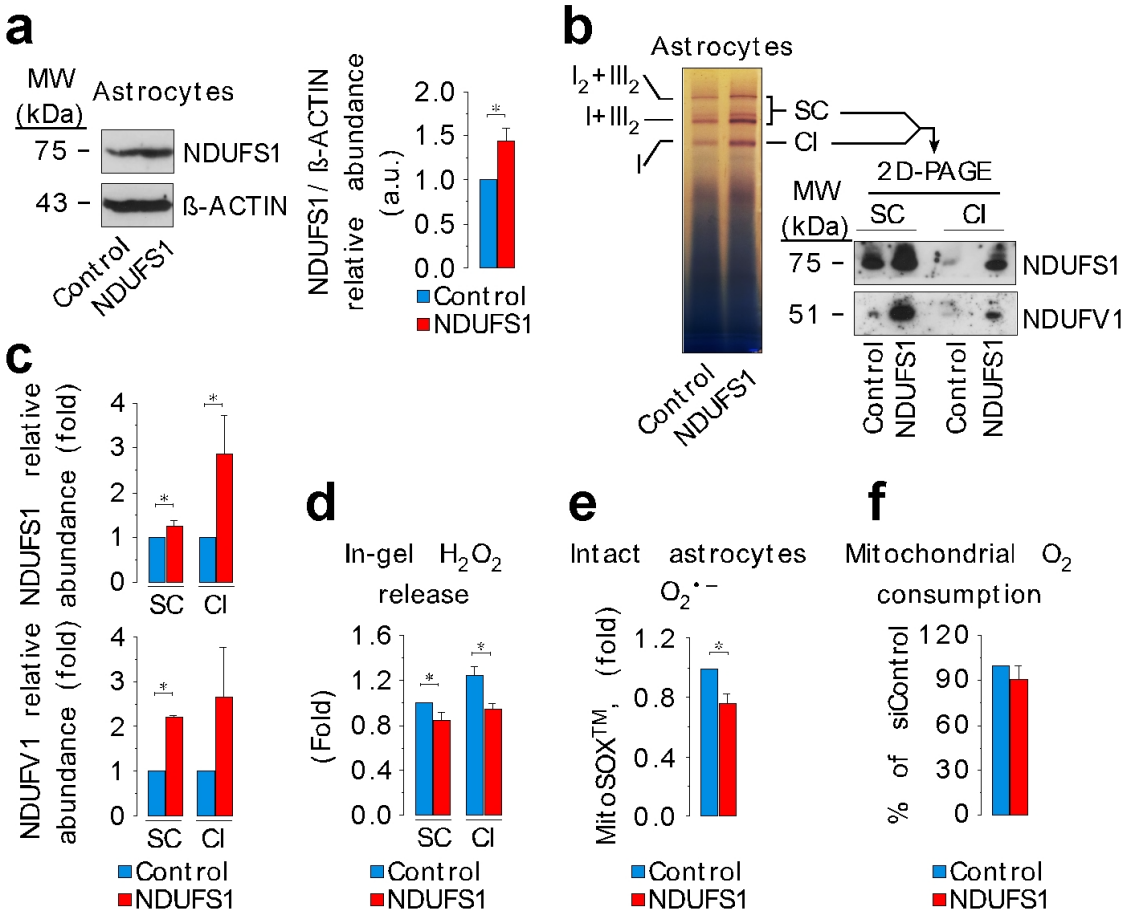

Fig. 4. NDUFS1 knockdown in neurons disassembles complex I from supercomplexes increasing ROS and impairing mitochondrial respiration

(*A*) Neurons were transfected with a siRNA against NDUFS1 (or a control siRNA) and, three days after, NDUFS1 protein abundance analyzed by western blotting in the whole cell extracts, followed by densitometric band quantification. ß-ACTIN was used as loading control. **(*B*)** Digitonin-solubilized isolated mitochondria from NDUFS1-

knocked down neurons were subjected to BNGE followed by in-gel complex I activity assay, and direct electro-blotting against complex I subunit NDUFS1, and complex III (UQCRC2) *plus* complex IV (MT-CO1). Bands corresponding to supercomplexes (SC) and free complex I (CI) were excised from the BNGE gel, and subjected to second dimension SDS-PAGE immunoblotting against NDUFS1 and NDUFV1. NDUFV1 abundance was assessed to distinguish between expression or stability of complex I. Coomassie stained proteins from the BNGE was used as loading control. **(*C*)** Densitometric quantification analyses of the NDUFS1 and NDUFV1 band intensities shown in panel b. **(*D*)** In-gel H_2O_2 production in the excised SC and CI bands from the BNGE of digitonin-solubilized isolated mitochondria from control and NDUFS1-knocked down neurons. H_2O_2 production values were normalized by the NADH dehydrogenase-activity band intensity obtained in the BNGE. **(*E*)** Mitochondrial ROS assessed using the MitoSox™ assay in intacts cells by flow cytometry. **(*F*)** Rate of pyruvate/malate (5 mM each; 1 mM ADP)-driven mitochondrial oxygen consumption in isolated mitochondria from neurons. CIII: complex III subunit UQCRC2; CIV: complex IV subunit MT-CO1. Data are the mean values ± S.E.M. from n=3-4 independent culture preparations (Student's t test). *$p<0.05$.

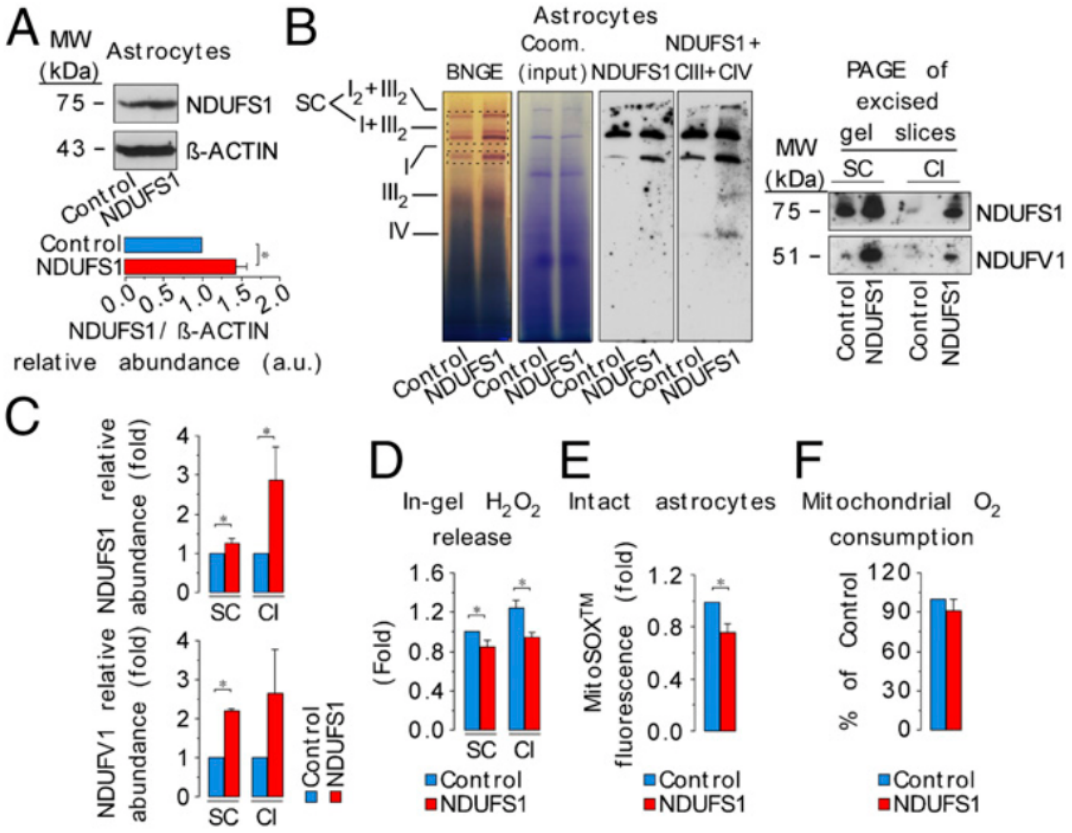

Fig. 5. Over-expression of NDUFS1 in astrocytes assembles complex I in supercomplexes and decreases ROS production

(*A*) Astrocytes were transfected with the full-length NDUFS1 cDNA (or control plasmid) and, 1 day after, NDUFS1 protein abundance analyzed by western blotting in the whole cell extracts, followed by densitometric band quantification. ß-ACTIN was used as loading control. **(*B*)** Digitonin-solubilized isolated mitochondria from NDUFS1-over-expressing astrocytes were subjected to BNGE followed by in-gel complex I activity assay, and direct electro-blotting against complex I subunit NDUFS1, and complex III (UQCRC2) *plus* complex IV (MT-CO1). Bands corresponding to supercomplexes (SC) and free complex I (CI) were excised from the BNGE gel, and subjected to second dimension SDS-PAGE immunoblotting against NDUFS1 and NDUFV1. Coomassie stained proteins from the BNGE was used as loading control. **(*C*)** Densitometric quantification analyses of the NDUFS1 and NDUFV1 band intensities

shown in panel b. **(*D*)** In-gel H_2O_2 production in the excised SC and CI bands from the BNGE of digitonin-solubilized isolated mitochondria from control and NDUFS1-over-expressing astrocytes. H_2O_2 production values were normalized by the NADH dehydrogenase-activity band intensity obtained in the BNGE. **(*E*)** Mitochondrial ROS as assessed using the MitoSox™ assay in intacts cells by flow cytometry. **(*F*)** Rate of pyruvate/malate (5 mM each; 1 mM ADP)-driven mitochondrial oxygen consumption in isolated mitochondria from astrocytes. CIII: complex III subunit UQCRC2; CIV: complex IV subunit MT-CO1. Data are the mean values ± S.E.M. from n=3-4 independent culture preparations (Student's t test). *$p<0.05$.